



On-line estimation and prediction of density and ethanol evolution in the brewery

Georges Corrieu, Ioan-Cristian Trelea, Bruno Perret

► To cite this version:

Georges Corrieu, Ioan-Cristian Trelea, Bruno Perret. On-line estimation and prediction of density and ethanol evolution in the brewery. Technical Quarterly, 2000, 37 (2), pp.173-181. hal-01537190

HAL Id: hal-01537190

<https://agroparistech.hal.science/hal-01537190>

Submitted on 16 Jun 2017

HAL is a multi-disciplinary open access archive for the deposit and dissemination of scientific research documents, whether they are published or not. The documents may come from teaching and research institutions in France or abroad, or from public or private research centers.

L'archive ouverte pluridisciplinaire **HAL**, est destinée au dépôt et à la diffusion de documents scientifiques de niveau recherche, publiés ou non, émanant des établissements d'enseignement et de recherche français ou étrangers, des laboratoires publics ou privés.

On-line estimation and prediction of density and ethanol evolution in brewery

Georges CORRIEU, Ioan Cristian TRELEA and Bruno PERRET
Laboratoire de Génie et Microbiologie des Procédés Alimentaires

INRA – INRA P-G, 78850 Thiverval-Grignon, France

Tél. 33 1 01 30 81 54 88 – Fax 33 1 01 30 81 55 97

email : corrieu@platon.grignon.inra.fr

Abstract

The fermentation rate, the wort density and the ethanol concentration are estimated on-line, based on the measurement of the CO₂ evolution rate. The future density evolution and the fermentation end-time are predicted using dynamic models based on neural networks and on the average fermentation kinetics. The decrease of the prediction error with time is demonstrated. The results are based on 33 industrial fermentations involving two sorts of beer. Implementation problems and practical difficulties are discussed.

Key words : CO₂ monitoring, density, fermentation end-time, neural networks, prediction.

Introduction

While more and more sophisticated equipment and methods are used for the supervision and control of fermentation tanks in brewery, the key operation which is the alcoholic fermentation, remains poorly understood and difficult to control. This comes from the lack of cheap and reliable sensors to measure the basic biological variables, such as the concentration of active yeast, residual sugars, ethanol and aroma compounds. At the dawn of the 21st century, brewers still use density measurements performed on manually taken samples. The on-line density measurement is still not operational in industry. The oscillating U-tube density meter [5] is expensive and difficult to clean.

The alternative consisting in the CO₂ measurement, also used in oenology (French patents n°86-15779 and n°87-4025430) was first proposed by Stassi *et al.* [9], and explored by different research teams, with various objectives. The reliable measurement of the released CO₂ is a critical issue, especially in an industrial context. Various kinds of flow meters, (mass, volumetric, Venturi tube) have been studied and compared [2,4,11,12]. In all cases, the mechanical design of the flow meter must allow easy cleaning and disinfection (French patent n°96-03823). Taking into account of the dissolved CO₂ fraction, depending on operating conditions (temperature, pressure, beer type, tank) increases the computation complexity without a noticeable accuracy gain. Pandiella *et al.* [8] recommend neglecting the dissolved CO₂ and correlating the density, the sugar and the ethanol concentrations directly to the released CO₂.

At present, it seems that mass flow meters and flow meters based on differential pressure measurement (French patent n°96-03823) are best suited for on-line monitoring of CO₂ evolution.

Linear relationships between the accumulated CO₂, the wort density, the sugar and ethanol concentrations are now well established [2,3,6,8,10]. However, regression parameters vary with experimental conditions such as the CO₂ measurement technique, the sort of beer, the fermentation process, the tank size and geometry. The models have to be determined separately for each application.

The released CO₂ measurement also allows real-time computation of the CO₂ production rate. A linear relationship has been shown to exist between the CO₂ production rate and the density drop rate [9]. Next, the relationships between the CO₂ production rate and the foam index have been established, as a function of operating conditions (wort, tank, process) [9,11]. Recently, analogies between the CO₂ and the heat production rates have been demonstrated experimentally, as well as correlations between the corresponding accumulated values [6,8]. All these studies confirm the importance of the measurement of the CO₂ production rate, which expresses the fermentation rate. However, this variable is still seldom used in brewery, as well as the automatic control approaches that it enables.

Thus, industrial tests conducted in France (Sebastian Artois Brewery) at the end of the 80's, using a single vortex flow meter connected successively to eight fermentation tanks, seem to have had no consequences. Yet they validated a control law associating the temperature, the pressure and the density evolution, and allowed a better CO₂ recovery [4].

The work of Gopal *et al.* [5] shows that the temperature control between 17 and 23°C allows one to follow an ideal gravity profile. Despite several restrictions (laboratory scale experiments; usage of an oscillating U-tube density meter, difficult to clean in industrial conditions; temperature control limited to cooling), the authors arrive at the conclusion that the approach would be useful at industrial scale.

The works reported by Stassi and coworkers are based on the measurement of the CO₂ production rate in order to control several important operating conditions:

1. Modification of the temperature set point in accordance with the fermentation rate, at laboratory scale [12].
2. Definition of a temperature profile which limits the maximum CO₂ production rate without augmenting the total fermentation time [11].
3. Optimization of the tank filling based on the foaming index [9,11].
4. Optimization of the released CO₂ recovery [9].
5. Design of a self-diagnosis system for the fermentation progress [9].

The automatic control of the fermentation process concerns mainly the cooling, even if other benefits may be expected, such as manpower, reproducibility and invariability of beer quality [8].

The present work has two goals. Firstly, it aims to confirm the linear relationships which allow us to estimate in real time the density and the ethanol evolution. Secondly, it presents two techniques for the prediction of the density evolution, in order to control the process dynamics and to manage the tanks immobilization, the cooling requirements, the filtering and bottling facilities, etc.

Materials and methods

Fermentation process

Experimental data were obtained from the Meteor brewery located at Hochfelden (France). Fermentation takes place in 300 m³ tanks (Figure 1) at variable temperature, comprised between 9 and 13°C. Two sorts of beer are considered : Pils and Export. Their initial wort density ranges from 9.3 to 11.8 Plato and the final density from 2.1 to 3.4 P. Tanks are inoculated at 5·10⁶ yeast/mL.

Instrumentation and supervision software

The temperature in the fermentation tank was measured with a platinum sensor ($100\ \Omega$ at 0°C) and was controlled using the cold water flow in the cooling jacket. The CO_2 release rate was computed based on a differential pressure measurement on a diaphragm (0–75 mbar sensor, model 1151 DP4 522B1, Rosemount).

The sensors were connected to a Johnson DC9000 process computer which carried out the analog/digital conversions with a 12 bit resolution. The data were transmitted every 10 seconds to a PC computer (486DX at 66 MHz) via RS422 serial link. The real-time multitasking supervision software BeerControl® averaged and stored the data every 30 minutes. It allowed a graphic representation of the fermentation process and performed all the computations involved in the density estimation and prediction.

Principle of the artificial neural networks

The neural network technology draws its analogy from the human brain. The brain is made of some 10^{11} highly interconnected neurons. It is believed that when information is stored in the brain, the synaptic strength of the connections between the neurons is modified. Similarly, in artificial neural networks, information is stored in the form of weights between artificial neurons. Each neuron is a simple processor which performs a weighted sum of all inputs from outside or from other neurons. The output of the neuron is obtained by passing the weighted sum through a nonlinear transfer function. For modeling physical systems, a layered feed-forward network is generally used. It consists of an input layer of neurons, an output layer, and one or more intermediate or hidden layers. The neurons in the input layer take their inputs from outside, while the other neurons take their inputs from the outputs of the neurons in the preceding layer.

When the network is created, the weights are initialized with random values. During the learning process, the weights are modified iteratively, such that the network responds with correct outputs in presence of known inputs. The input-output pairs used in the learning process form the learning database. When the error between the network outputs and the known correct outputs is sufficiently small, the learning is stopped and the generalization ability is tested by estimating the prediction error on previously unseen examples, which form the test database. If the performance is considered satisfactory, the network is ready for use in applications. Otherwise, the learning process is restarted with different random initial weights or different numbers of neurons in the hidden layers.

Artificial neural networks received a great deal of attention in recent years. Theoretical properties of the networks have been established rigorously, relative advantages of various architectures (e.g. number of hidden layers or type of transfer function) have been investigated and efficient learning algorithms have been proposed. For a concise introduction to this subject, the interested reader may consult for example the work of Bishop [1]. New books on neural networks are published every year and software vendors propose various hands-on packages.

Mathematically, neural networks are analogous to other universal function approximators, such as polynomials and Fourier series. For example, any function can be approximated arbitrary well by a superposition (weighted sum) of polynomials, up to a sufficiently high order: 1, x , x^2 , x^3 , x^4 , etc. The Fourier decomposition uses harmonic functions instead of polynomials: 1, $\cos x$, $\sin x$, $\cos 2x$, $\sin 2x$, $\cos 3x$, etc. Most neural networks use sigmoid (that is monotonic and bounded) transfer functions, such as hyperbolic tangent or $1/(1+\exp x)$. The main difference with traditional function approximators is that the basis functions are not fixed, like in the case of polynomials and Fourier series, but adaptive, i.e. depend on the network weights and hence on the problem being solved. This has several consequences: (1) Statistically, less coefficients are needed for a given degree of accuracy, especially if the number of input variables is high. (2) Interpolation between known data points is smoother; (3) The determination of the network weights (the learning process) is more difficult. Examples of functions realized as weighted sums of sigmoids are given in Figure 2.

Dynamic neural network model

In order to express the progress of the fermentation, we use a dimensionless variable, a , called the "progress factor", which can be related to the wort density, D , to the released CO_2 , C , to the ethanol concentration, E , and to the residual sugar concentration, S :

$$a(t) = \frac{D_i - D(t)}{D_i - D_f} = \frac{C(t)}{C_f} = \frac{E(t)}{E_f} = \frac{S_i - S(t)}{S_i} \quad (\text{Eq. 1})$$

Here t is the current time, the index i refers to the initial value and the index f to the final (asymptotic) value. For every sort of wort, the initial density, D_i , is measured before the fermentation begins and the final density, D_f , is determined from a laboratory test. The total amount of CO_2 released, C_f , and the final ethanol concentration, E_f , are determined from D_i using linear correlations. The current amount of CO_2 , $C(t)$, is measured on-line.

The dynamic prediction model (Figure 3) is a neural network with two inputs, the relative progress factor and the wort temperature at the current time, two hidden neurons and one output, representing the predicted relative fermentation progress one step ahead. The time step is equal to 2 hours. In order to obtain long time predictions (typically up to the end of the batch), the computed progress factor is recursively introduced at the network input [7]. The temperature profile must be known in advance, which is the case for the considered brewery. The 13 network coefficients were determined using 22 randomly selected fermentation experiments, which formed the learning database. Network coefficients were initialized randomly and were optimized with a Quasi-Newton algorithm aiming at a minimum sum-squared prediction error. The remaining 11 experimental runs formed the test database, and were used for the selection of the network with the best generalization ability among the various structures (1 to 6 hidden neurons) and various random initial coefficient sets.

Dynamic model based on the average fermentation kinetic

The kinetic model was developed in order to exploit additional information available on-line, which could not been taken into account by a purely "black box" approach like a neural network, but which proved useful for improving the accuracy of the predictions. It turned out that some fermentations were consistently slower or faster than the average. This difference could not be explained by the temperature effect, but could be detected early enough to be corrected for during the rest of the fermentation.

The effect of the wort temperature on the fermentation rate, $f_1(T)$, was determined by separate laboratory experiments and expressed as an acceleration or a slowdown factor with respect to the same fermentation rate at 10°C. An average fermentation kinetic at 10°C was determined from the available industrial data after compensation for the temperature effect, and the resulting empirical function was called $f_2(a)$. No analytic expression was fitted for $f_2(a)$, but its values were tabulated for values of a between 0 and 1 and interpolated if required.

The dynamic model can be written in state-space form as:

$$\frac{da(t)}{dt} = z \cdot f_1(T(t)) \cdot f_2(a(t)) \quad (\text{Eq. 2})$$

$$a(0) = 0 \quad (\text{Eq. 3})$$

Here z is a global acceleration coefficient to be estimated on line. Let t_p denote the present moment and a_{mes} the measured progress factor (based on the amount of CO₂ released, Eq. 1).

The acceleration coefficient, z , is computed aiming at the best possible agreement between the simulated and the measured progress factor:

$$z = \arg \min \left(a(t_p) - a_{mes} \right)^2 \quad (\text{Eq. 4})$$

The estimated value of z is used for prediction until a new estimation is made, based on a new measurement of the progress factor.

Results and discussion

Typical fermentation

A typical evolution of the process variables is shown in Figure 4, for a Pils beer production. The temperature is maintained around 10°C during the first two days, than gradually risen to 13°C and maintained until the end of the fermentation. When the CO₂ production rate falls down near zero, the tank is cooled to about 5°C and emptied.

The measurement of the CO₂ production rate is very noisy, despite the preprocessing with a moving average filter (180 data points acquired every 10 seconds are averaged together to give one measurement every 30 minutes). The large spikes in the CO₂ production rate curve are due to commutation of the CO₂ recovery device. The maximum production rate (0.18 m³/m³.h) is obtained when the temperature is stabilized at its maximum value (13°C). The final decrease of the production rate is due to sugar limitation.

Density measurements are obtained every day. Our goal is to replace manual sampling by indirect measurement based on CO₂ production.

On-line density and ethanol estimation

The wort density and the ethanol concentration are estimated on-line from the accumulated amount of the evolved CO₂ using linear correlations, as follows from Eq. 1. Experimental data used for establishing the correlations are shown in Figure 5. The correlation between CO₂ and density variation was established using 8 fermentations (Figure 5A). When applied to the 33 available fermentations, for a total of 241 density measurements, the mean estimation error was of 0.27 P, which is of the same order as the density measurement accuracy. The available ethanol concentration measurements are limited to 3 fermentations (Figure 5B). The mean error is 0.12 mL/100mL.

The on-line density estimation is illustrated in Figure 6, for the two considered sorts of beer. In Figure 6A, all estimation errors are small (maximum error 0.16 P, mean error 0.06 P), while in Figure 6B the estimation error for the second sample is quite large (maximum error 0.75 P, mean error 0.23 P). The large error in Figure 6B is probably due to incorrect initial density measurement. Density measurement errors occasionally occur due to incorrect readings of the pycnometer. This is particularly apparent in the final fermentation phase, when some experimental values are slightly higher than the preceding ones, which is obviously not possible from a physical point of view.

Density and fermentation end time prediction using neural network

The neural network was used to predict the fermentation progress factor (and hence the density and the fermentation end time) starting at moments where the progress factor was known via the CO₂ measurement. The measured value was used to initialize the network, and the prediction up to the end of the batch was carried out in a recurrent manner, with a 2 hours time step.

The fermentation end time is defined as the moment when the progress factor reaches 0.95 (that is, 95% of the CO₂ is released or 95% of the density variation is accomplished). This threshold was adopted because in practice it is impossible to determine the moment when the progress factor reaches 1 accurately enough. The convergence to this value is asymptotic and small CO₂ measurement errors give huge errors in the end time determination. From a practical point of view, it is possible to add a constant value (say 12 hours) to the end time defined by $\alpha = 0.95$ in order to consider that the fermentation is completely finished. The addition of a constant value does not change the prediction errors given below.

Examples of the prediction procedure applied to three different fermentations are shown in Figure 7. In Figure 7A the results are excellent from the start, Figure 7B is a typical situation, while in Figure 7C the accuracy is relatively poor. In all cases, the prediction accuracy improves with time, when the network is initialized with a higher progress factor.

The results for all the 33 available fermentations are summarized in Figure 8. The prediction error, for both the density and the end time, decreases with time. From a progress factor of 0.5, the density is predicted with a mean error less than 0.2 P and the end time with a mean error less than 5 hours, which is considered satisfactory for an average fermentation time of 4 days (5%).

Density and fermentation end time prediction using the average kinetic

In situations like the one represented in Figure 7C, the predicted evolution is systematically slower (and in some cases faster) than the true one, but this behavior can not be explained through the measured operating conditions like the temperature and the initial wort density. Possible causes are variations in the inoculum concentration, in the yeast strain or its physiological state, in wort composition (like concentration of aminoacids) etc., but these variables are usually not measured. The kinetic model allows us to determine the global slowdown or acceleration factor at relatively early stages of the fermentation and thus improve subsequent predictions.

The Meteor brewery systematically uses a temperature profile like the one presented in Figure 4, and in all our data the temperature is highly correlated with the progress factor. In order to determine the temperature effect alone, separate laboratory experiments were performed, giving the result represented in Figure 9. For each fermentation, the progress rate da/dt was computed from the measured CO_2 evolution rate dC/dt and Eq. 1 and compensated for the temperature effect, giving an equivalent progress rate at 10°C, shown in Figure 10. The values of the average progress rate were tabulated for 21 values of the progress factor, as indicated in Table 1. The average progress rate was used in the kinetic model described by Eq. 2. Interpolation was performed if intermediate values were required.

When the fermentation is in progress, the global acceleration factor can be determined from Eq. 4 and the measured CO_2 . Using this factor for subsequent predictions results in significant accuracy improvement, as illustrated in Figure 11 by the same fermentation as in Figure 7C. At the beginning, no additional information is available and the acceleration factor is taken as $z = 1$, which results in a large prediction error. As soon as the progress factor reaches 0.25, better estimates of z become available and the systematic error visible in Figure 7C disappears.

The prediction error on the whole data set is summarized in Figure 8. The mean error is lower than in the case of the neural network, mainly because of the on-line estimation of the acceleration factor.

Practical implementation considerations

During the industrial implementation phase, several precautions must be taken in order to achieve the stated measurement and prediction accuracy. Some of them might seem trivial to

people used to laboratory conditions, but they can make the difference between the success or the failure of an industrial project.

Zero of the differential pressure sensor. The CO₂ evolution rate dC/dt (in m³ of CO₂ per m³ of wort and per hour) is estimated from a differential pressure measurement Δp (in mbar) using the Eq. 5 :

$$\frac{dC}{dt} = \frac{k}{V_{wort}} \text{sign}(\Delta p) \sqrt{|\Delta p|} \quad (\text{Eq. 5})$$

The total wort volume V_{wort} is in m³ and the constant depends on the diaphragm design (it was $k = 6 \text{ m}^3 \cdot \text{h}^{-1} (\text{mbar})^{-1/2}$ in our case). The square root function has an infinite slope near zero, which means that a very small offset in the differential pressure measurement results in a quite large offset in the CO₂ release rate. An example that actually occurred in our experiments is shown in Figure 12. The units for the pressure drop and for the CO₂ release rate are selected in order to give similar signal amplitudes at the figure scale. It can be seen that an apparently negligible offset in the pressure drop measurement completely jeopardizes the measurement of the released CO₂.

Wort volume measurement. The volume of the released CO₂ is expressed per unit of wort volume. An error in the wort volume measurement in Eq. 5 results in an error in the progress factor estimation, since the total amount of the CO₂ to be released per m³ of wort (C_f in Eq. 1) is related to the initial wort density and is computed in advance. Errors in the progress factor estimation are particularly harmful for the final fermentation time prediction, as illustrated by the dotted line in Figure 8. The prediction algorithm based on the average kinetic was applied, replacing the true value of the wort volume V_{wort} by a value affected by random normally distributed 5% measurement error. The final time prediction error never decreases below 4 hours, and even increases for progress factors larger than 0.75.

Conclusions

Indirect measurement of wort density and ethanol concentration are implemented in the BeerControl® supervision software and are in everyday use at the Meteor brewery. Collected data was used for establishing predictive dynamic models of the fermentation process. The feasibility of on-line predictions of both wort density evolution and fermentation end time, based on the measurement of the CO₂ evolution rate, is demonstrated.

Two kinds of dynamic models were developed and compared. The neural network model requires only a limited number of elementary arithmetic operations and can be readily

incorporated in the existing supervision software. However, it can not take into account the fact that certain fermentations are systematically faster or slower than predicted, even if this information becomes available at an early stage. This drawback is eliminated by the model based on the average fermentation kinetic, but its implementation requires more sophisticated numerical tools: an ordinary differential equation solution and optimization in a one-dimensional space.

In the case of indirect density measurement, the average error is 0.27 P, and in the case of indirect ethanol measurement, 0.12 mL/100mL. The prediction error decreases with time for both dynamic models. When the released CO₂ exceeds half of the total expected amount (known in advance from the initial density measurement), the density evolution can be predicted with a mean error of 0.18 P using the neural network and 0.15 P with the kinetic model. The fermentation end time, defined as the moment when 95% of the CO₂ has been released (plus a constant delay of 12 hours), can be predicted with a mean error of 4.75 and 2.5 hours respectively.

The stated accuracy is satisfactory for practical purposes, but several precautions have to be taken to achieve it in industry. The final wort density must be known in advance. It can either be determined with a relatively quick (24 hours) laboratory test, or inferred from the initial wort density and past experience with the considered wort type. The total CO₂ to be released must also be known in advance, which means that the initial wort density and the wort volume must be measured accurately (say, better than 0.05 P for the wort and 1% for the volume). If the CO₂ release rate is estimated from the measurement of a pressure drop over a diaphragm (as in the considered brewery), the offset of the differential pressure sensor must be compensated very carefully, because its effect is exacerbated by the square-root relationship between the pressure and the flow rate.

Acknowledgments

The authors wish to thank the French Ministère de l'Enseignement Supérieur et de la Recherche, the Meteor brewery and the Institut Français de la Brasserie et de la Malterie for their financial and/or technical support.

References

1. BISHOP, C.M. (1994). Neural network and their applications, *Rev. Sci. Instrum.*, Vol. 65, pp. 1803-1832.
2. DAOUD, I. S., DYSON, R., IRVINE, J. and CUTHBERTSON, R.C. (1989). Practical experience of on-line monitoring of evolved CO₂ from production fermenters, *Proceedings of the 22nd European Brewing Convention*, Zurich, Germany, pp. 323-330.
3. DAOUD, I. S. and SEARLE, B. A. (1990). On-line monitoring of brewery fermentation by measurement of CO₂ evolution rate, *Journal of Institute of Brewing*, Vol. 96, pp. 297-302.
4. EYBEN, D. (1989). An automated method for fermentation process control, *MBAA Technical Quarterly*, Vol. 26, pp. 51-55.
5. GOPAL, C.V., HAMMOND, J.R.M., and PYE, J.M. (1993). Interactive control of beer fermentation: Demonstration at the laboratory scale, *MBAA Technical Quarterly*, Vol. 30, pp. 71-79.
6. MILLER, J., PATINO, H., BABB, M. and MICHENER, W. (1995). Comparison of exotherm and carbon dioxide measurements in brewing fermentations, *MBAA Technical Quarterly*, Vol. 31, pp. 95-100.
7. NARENDRA, K.S. and PARTHASARATHY, K. (1990). Identification and control of dynamic systems using neural networks, *IEEE Transactions on Neural Networks*, Vol. 1, pp. 4-26.
8. PANDIELLA, S., GARCIA, L., DIAZ, M. and DAOUD, I.S. (1995). Monitoring the carbone dioxide during beer fermentation, *MBAA Technical Quarterly*, Vol. 32, pp. 126-131.
9. STASSI, P., RICE, J.F., MUNROE, J.H. and CHICOYE, E. (1987). Use of CO₂ evolution rate for the study and control of fermentation, *MBAA Technical Quarterly*, Vol. 24, pp. 44-50.
10. STASSI, P., RICE, J., KIECHEFFER, T. and MUNROE, J. (1989). Control of fermentation foaming using temperature profiling, *MBAA Technical Quarterly*, Vol. 26, pp. 113-122.

11. STASSI, P., GOETZKE, G. and FEHRING, J. (1991). Evaluation of an insertion thermal mass flowmeter to monitor CO₂ evolution rate in plant scale fermentation, MBAA Technical Quarterly, Vol. 28, pp. 84-88.
12. STASSI, P., FEHRING, J., BALL, C., GOETZKE, G. and RYDER, D. (1995). Optimization of fermentor operations using a Fermentor Instrumentation System, MBAA Technical Quarterly, Vol. 32, pp. 57-65.

Table 1

Experimental average fermentation kinetic.

Progress factor	0	0.05	0.10	0.15	0.20	0.25	0.30	0.35	0.40	0.45	0.50
Progress rate [10^{-4}h^{-1}]	26	62	77	79	87	92	94	99	104	104	103

Progress factor	0.55	0.60	0.65	0.70	0.75	0.80	0.85	0.90	0.95	1
Progress rate [10^{-4}h^{-1}]	105	104	103	101	98	95	89	80	51	0

LIST OF FIGURES

Figure 1. Industrial fermentation tank.

Figure 2. Principle of feed-forward neural networks. **(A)** Function of one variable (top), realized as a sum of three sigmoids (bottom). This corresponds to a neural network with one input, one hidden layer with three neurons and one output. **(B)** Function of two variables (top), realized as a sum of three sigmoids (bottom). This corresponds to a neural network with two inputs, one hidden layer with three neurons and one output.

Figure 3. Neural network structure. The network consists of layers of interconnected units (neurons). Each neuron in the hidden layer computes a weighted sum of the network inputs and transforms it using a "squashing" (sigmoid) nonlinear function. The single neuron in the output layer computes a weighted sum of the outputs of the hidden layer and transforms it using the sigmoid function.

Figure 4. Typical evolution of the process variables for a Pils beer production.

Figure 5. Linear correlations. **(A)** Density variation $D_i - D(t)$ as a function of the cumulated amount of the evolved CO₂. Data from 4 Pils and 4 Export beer productions. Determination coefficient $R^2 = 0.986$. **(B)** Ethanol concentration as a function of the accumulated amount of the evolved CO₂. Data from 1 Pils and 2 Export beer productions. Determination coefficient $R^2 = 0.987$.

Figure 6. Examples of on-line density estimation from CO₂ measurement. Data not used for establishing the correlation. **(A)** Pils beer, maximum error 0.16 P, mean error 0.06 P. **(B)** Export beer, maximum error 0.75 P, mean error 0.23 P.

Figure 7. Examples of predictions using the neural network. Predictions begin at progress factors of 0 (—), 0.25 (●●●), 0.5 (— - —), 0.75 (- - -) and 0.9 (— — —). **(A)** Very good

accuracy from the start. **(B)** Typical situation. **(C)** Predicted evolution systematically slower than the true one. Density samples (\bullet), measured CO₂ (—), density and CO₂ predictions and fermentation end time for $a = 0.95$ (|).

Figure 8. Evolution of mean prediction errors with fermentation time.

Figure 9. Ratio of progress rate at a given temperature to the progress rate at 10°C.

Figure 10. Progress rate at 10°C as a function of the progress factor. The progress rate is determined from the CO₂ production rate measurements.

Figure 11. Example of prediction using the average fermentation kinetic. The same experimental data as in Figure 6C. Predictions begin at progress factors of 0 (—), 0.25 (•••), 0.5 (— - —), 0.75 (- - -) and 0.9 (— —). When the progress factor reaches 0.25, a global acceleration factor is estimated and used for prediction. The systematic error disappears. Density samples (o), measured CO₂ (—), density and CO₂ predictions and fermentation end time for $a = 0.95$ (|).

Figure 12. The importance of the differential pressure offset compensation. **(A)** A small offset in the pressure drop measurement results in a large offset in the CO₂ release rate measurement, due to the square root relationship. **(B)** Accurate offset compensation.

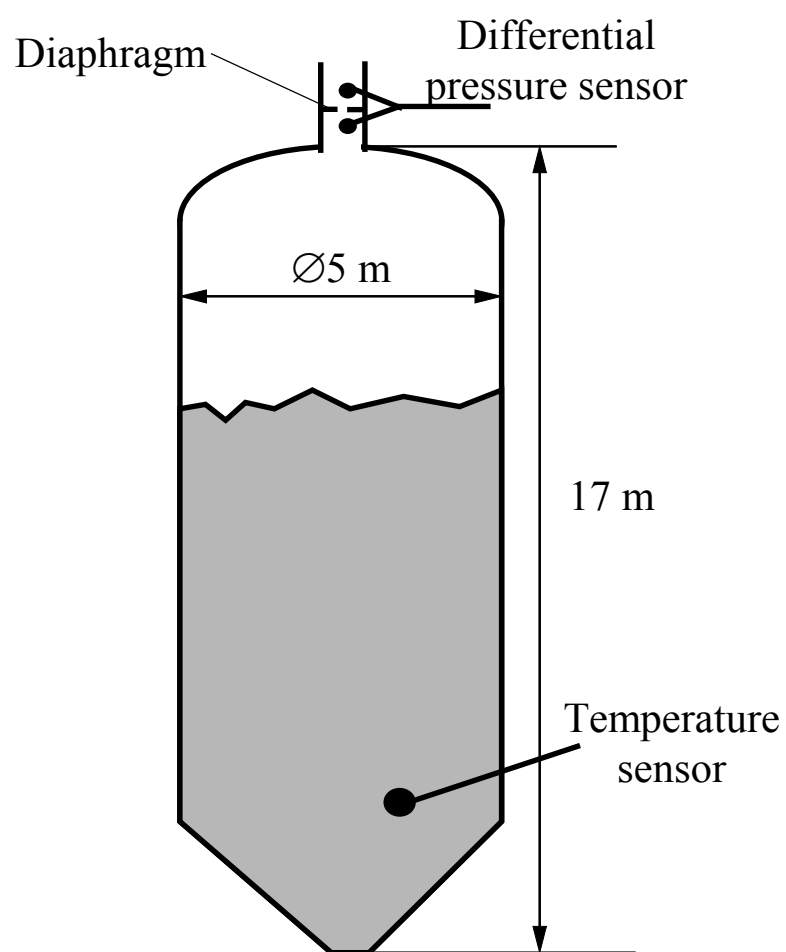


Figure 1

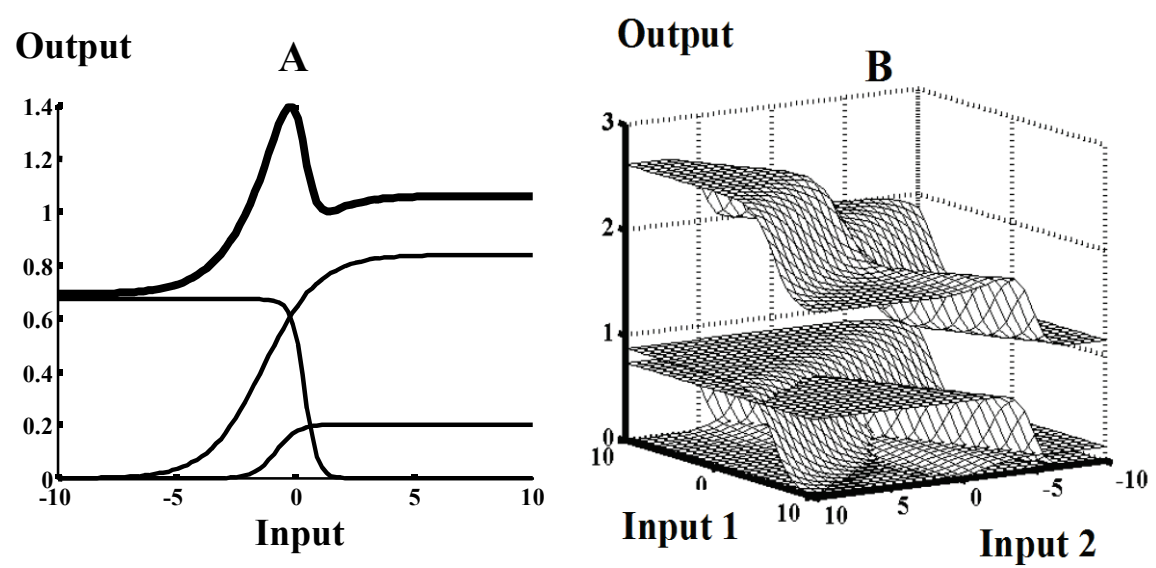


Figure 2

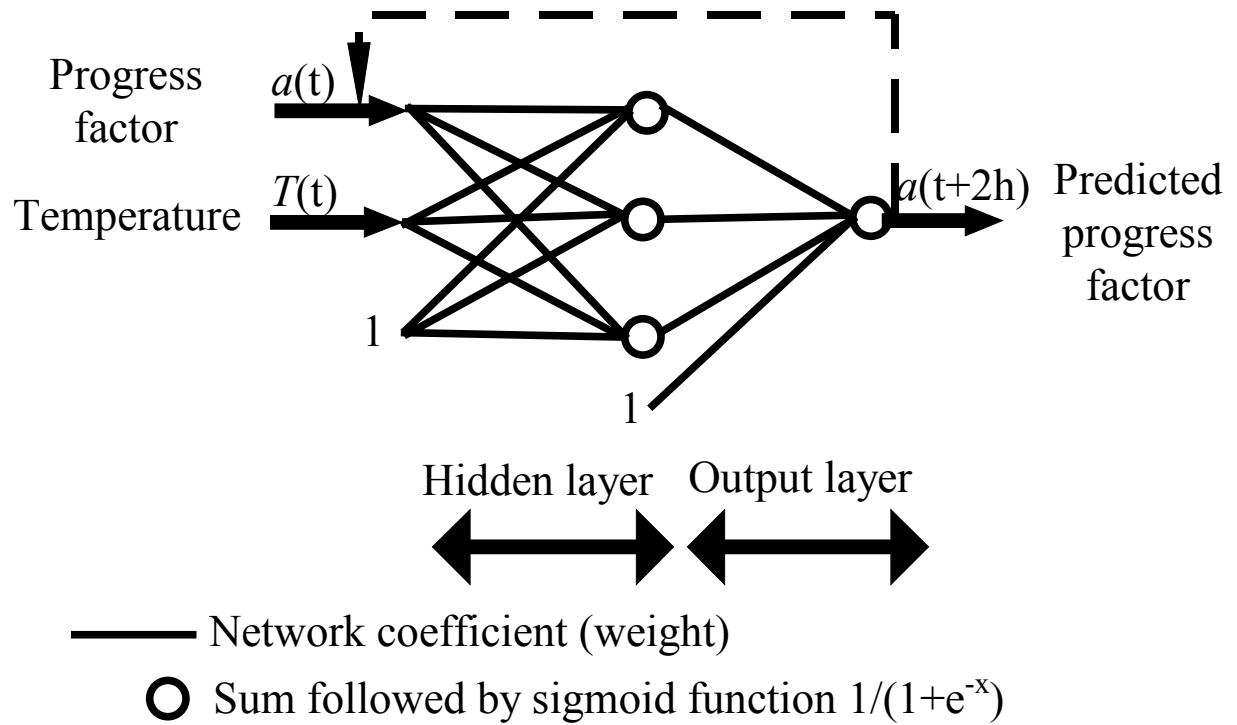


Figure 3

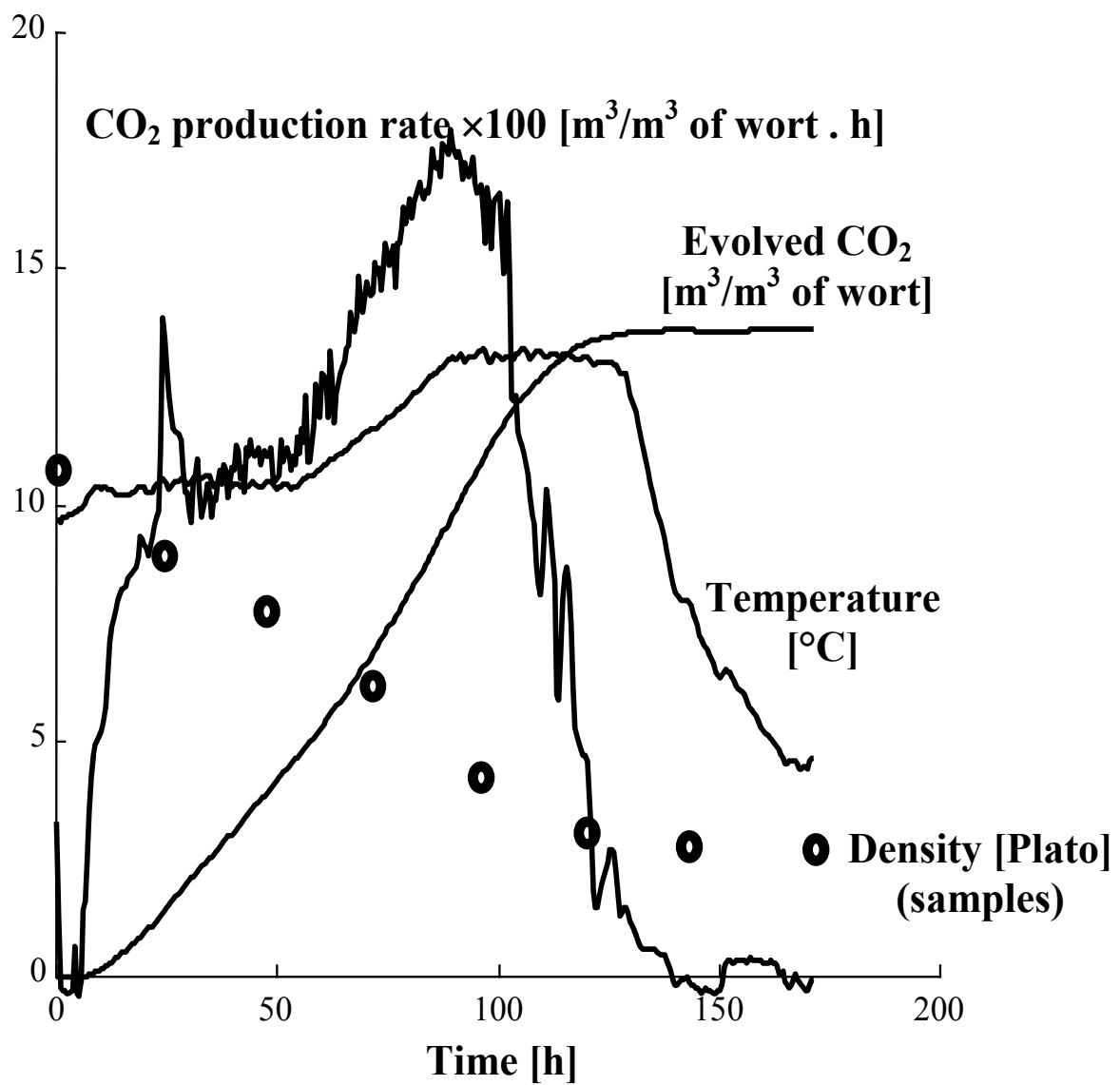


Figure 4

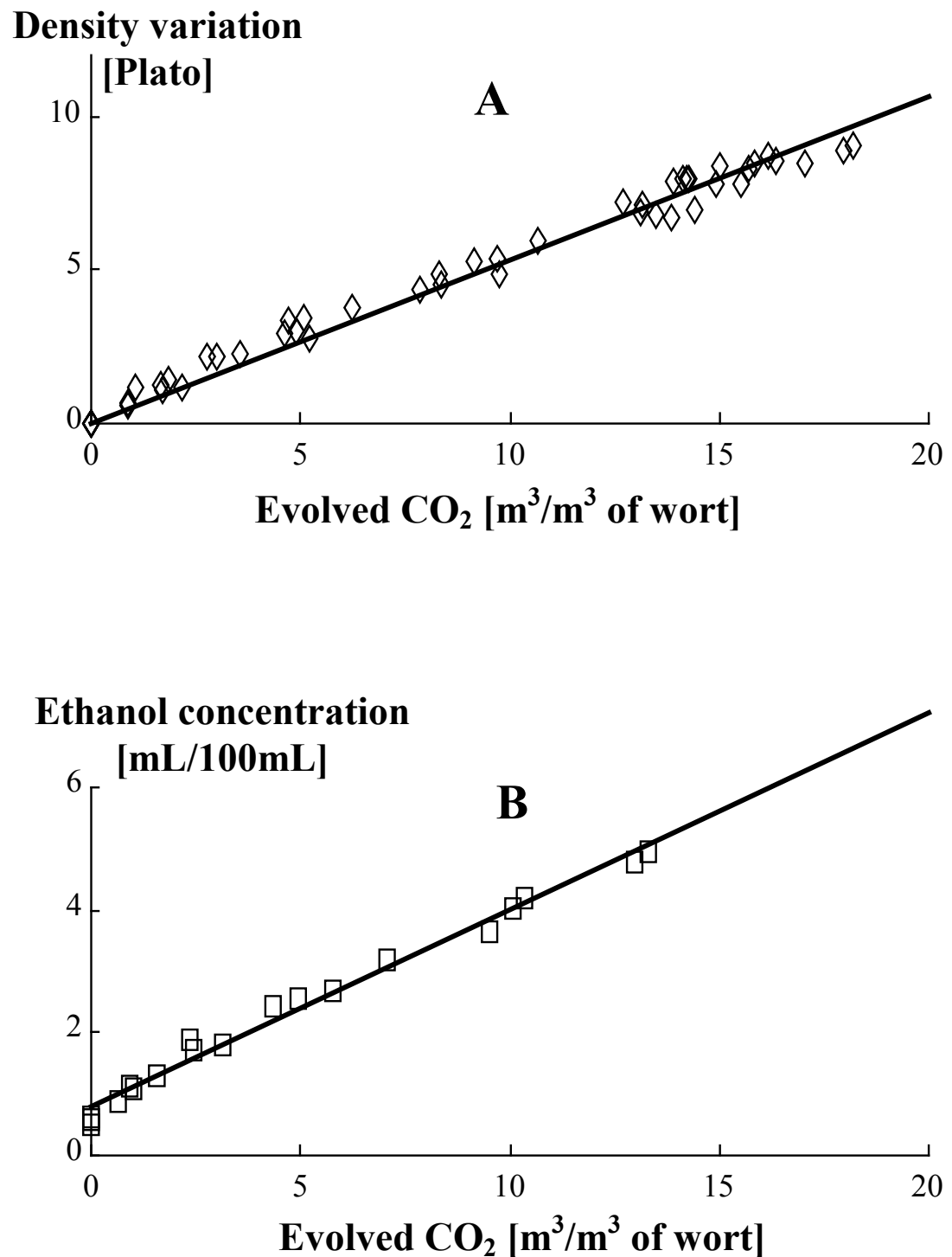


Figure 5

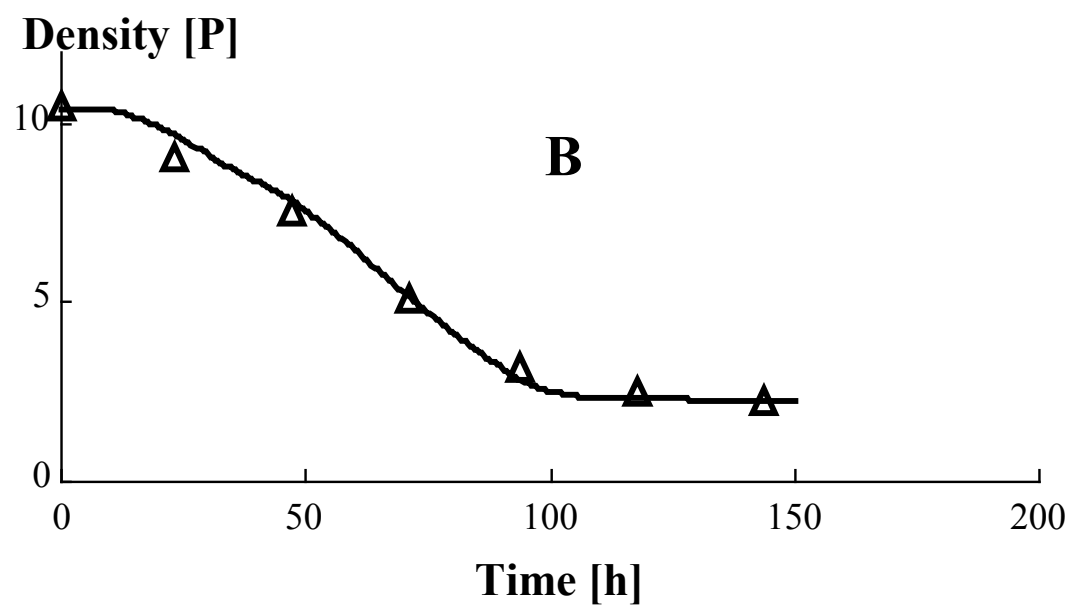
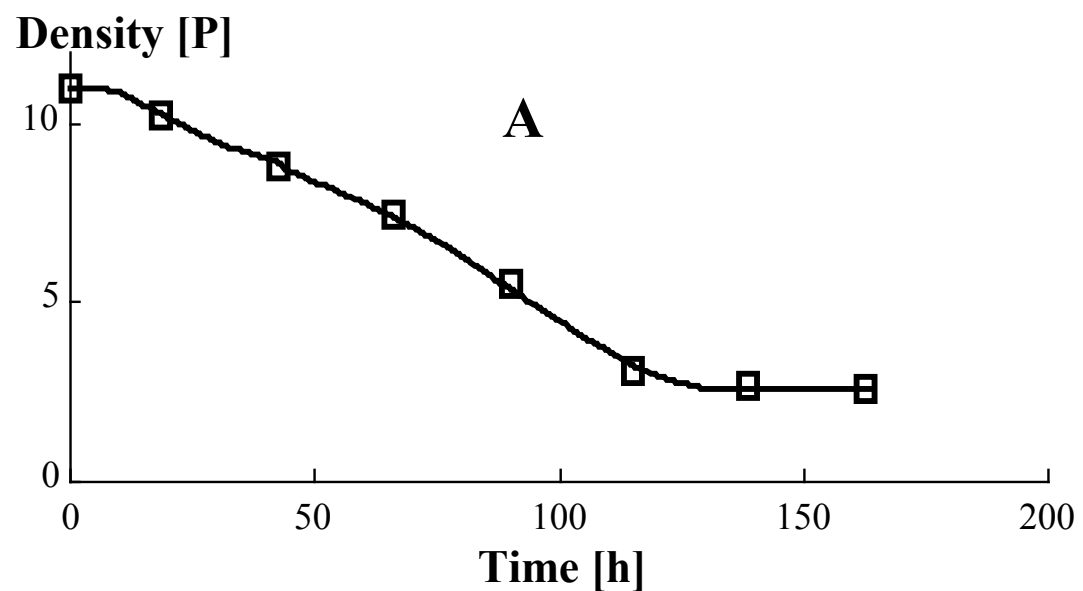


Figure 6

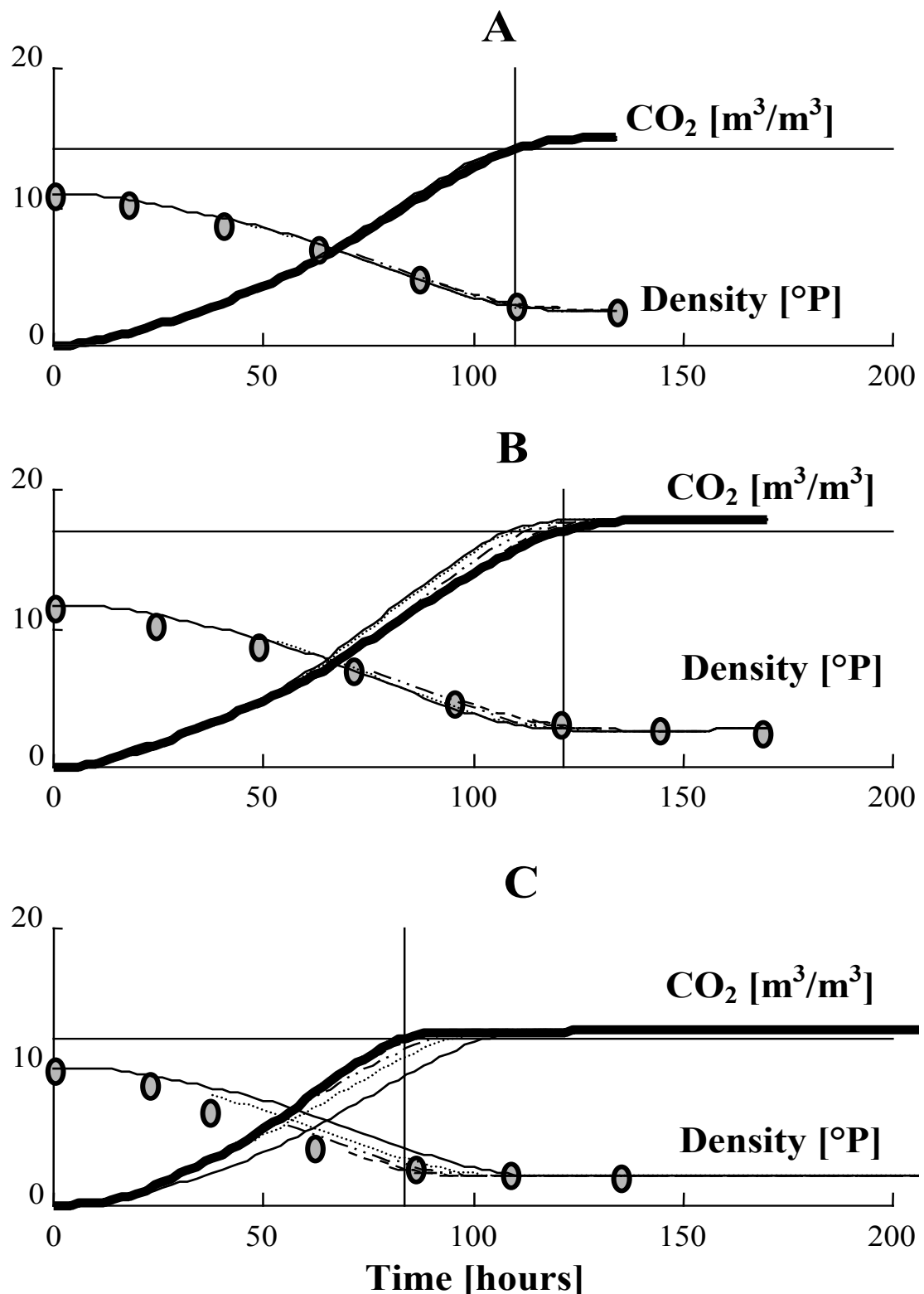


Figure 7

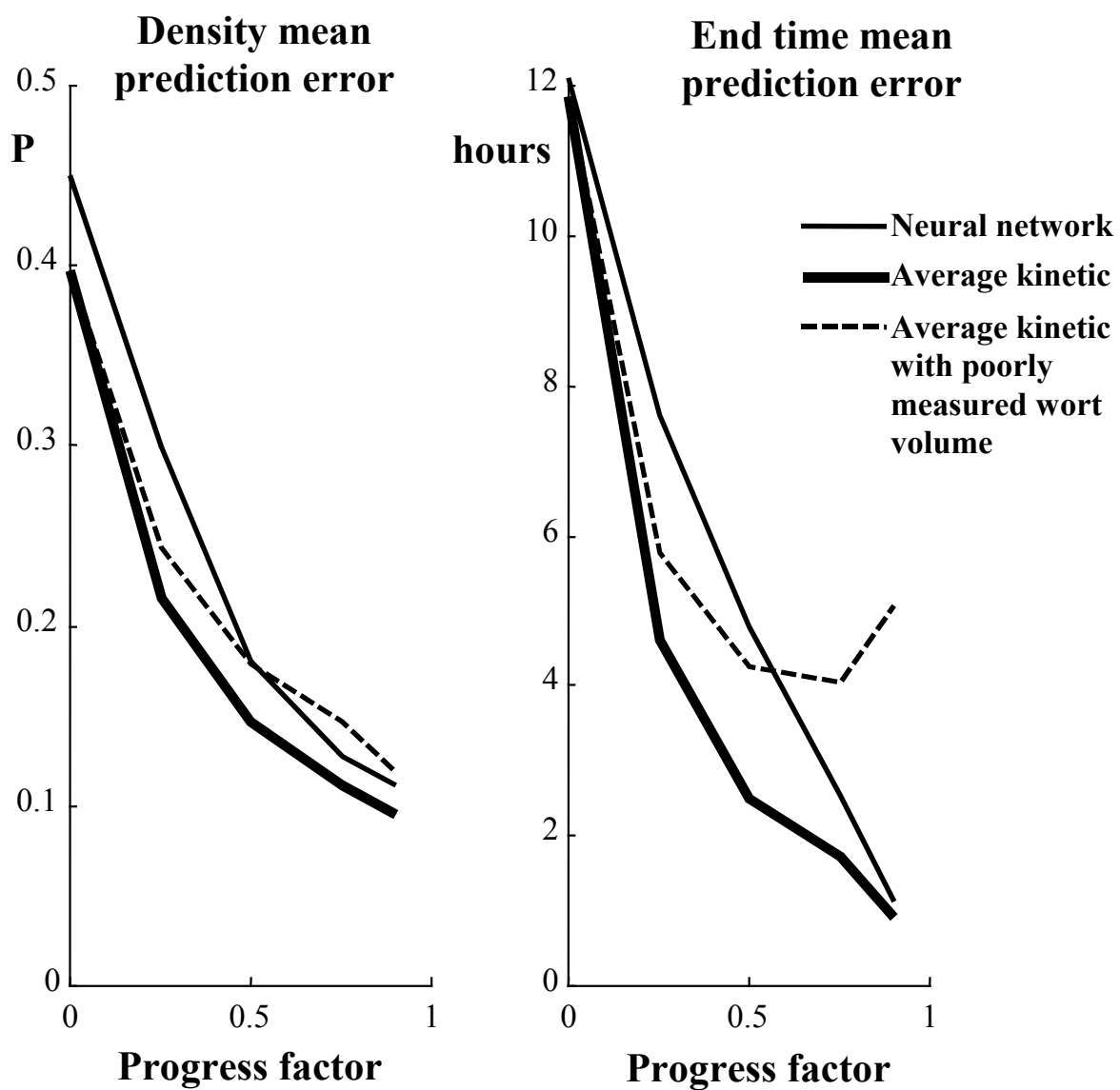


Figure 8

Progress rate ratio

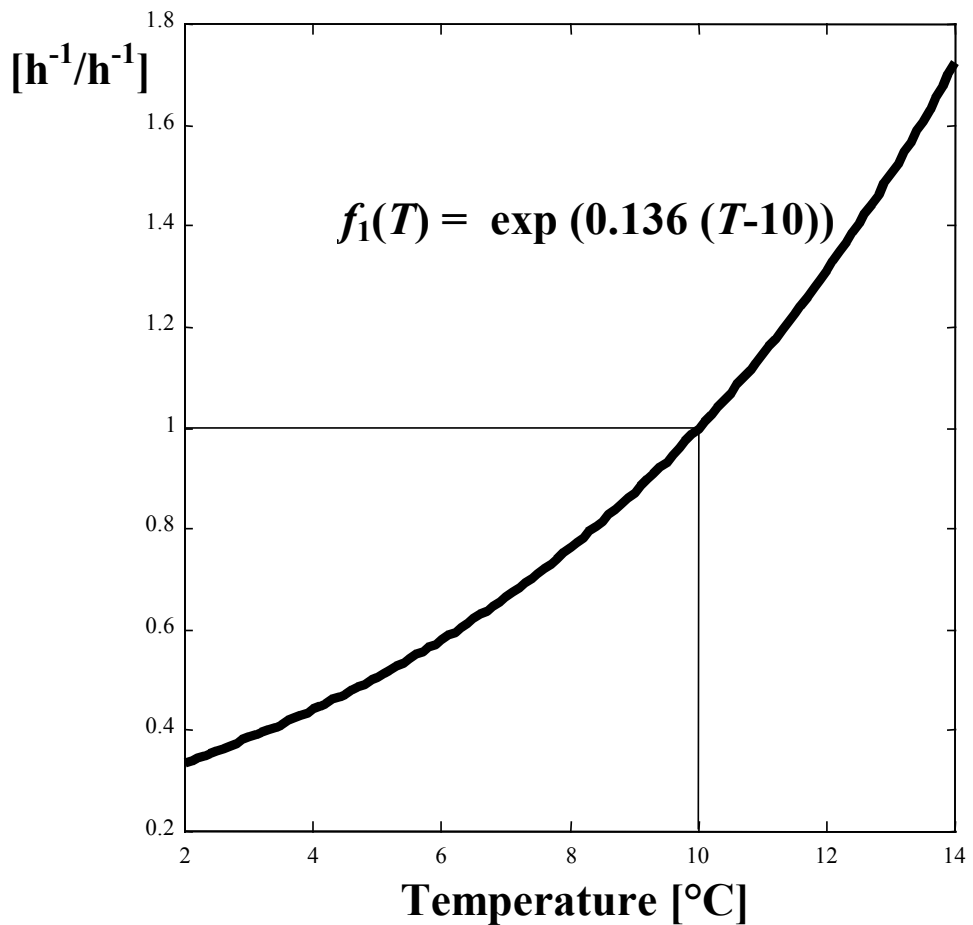


Figure 9

Progress rate

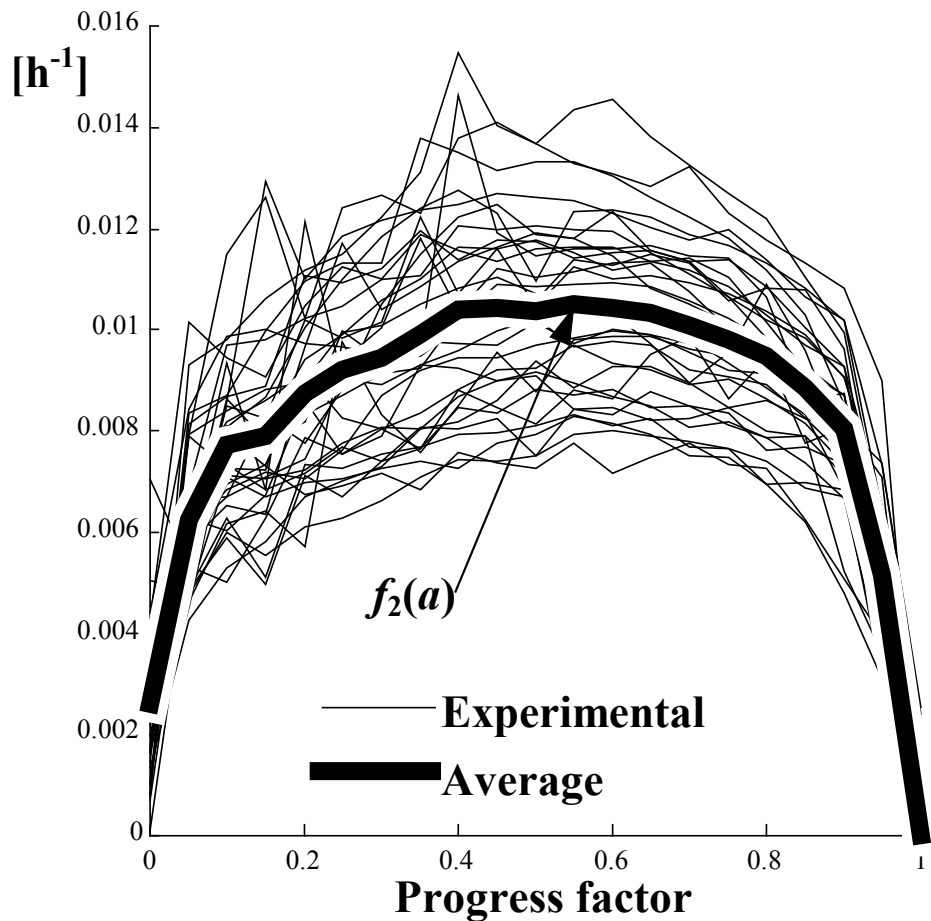


Figure 10

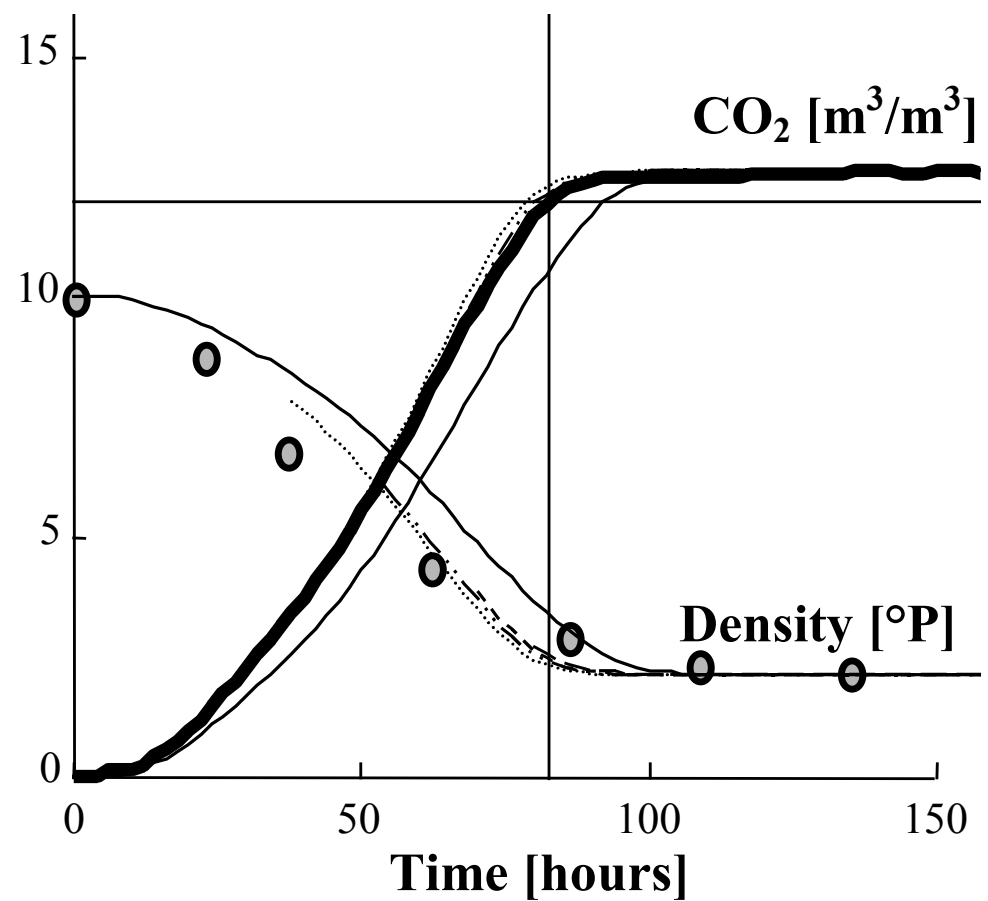


Figure 11

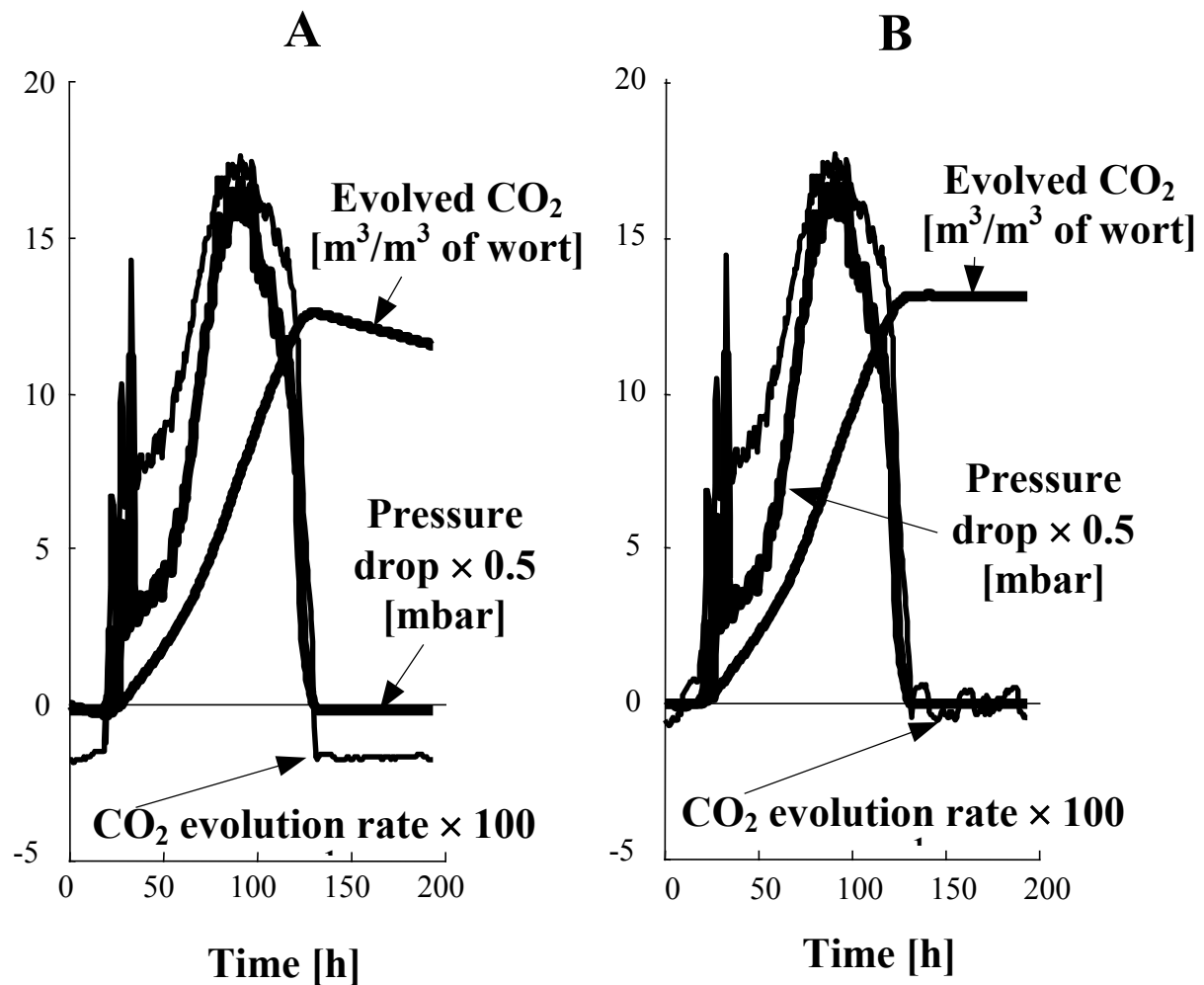


Figure 12